



BIREFRINGENT DIRAC FERMION IN ANISOTROPIC VELOCITY  
MODULATED GRAPHENE JUNCTION

MR. EAKKARAT PATTRAWUTTHIWONG

A THESIS SUBMITTED IN PARTIAL FULFILLMENT OF THE REQUIREMENTS  
FOR THE DEGREE OF MASTER OF SCIENCE (PHYSICS)  
FACULTY OF SCIENCE  
KING MONGKUT'S UNIVERSITY OF TECHNOLOGY THONBURI  
2020

Electronic Transport of Dirac Fermion in Tilted Velocity Modulated Dirac  
Material Junction

Mr. Eakkarat Pattrawutthiwong B.Sc. (Applied Physics)

A Thesis Submitted in Partial Fulfillment of the Requirements for  
the Degree of Master of Science (Physics)

Faculty of Science

King Mongkut's University of Technology Thonburi

2020

Thesis Committee

..... Chairman of Thesis Committee  
(Asst. Prof. Thana Sutthibutpong, Ph.D.)

..... Member and Thesis Advisor  
(Asst. Prof. Watchara Liewrian, Ph.D.)

..... Member  
(Lect. Tanapat Deesawan, Ph.D.)

..... Member  
(Lect. Suwat Tangwancharoen, Ph.D.)

Copyright reserved

Thesis Title      Electronic Transport of Dirac Fermion in Tilted Velocity  
Modulated Dirac Material Junction

Thesis Credits    12

Candidate        Mr. Eakkarat Patrawutthiwong

Thesis Advisor    Asst. Prof. Watchara Liewrian

Program          Master of Science

Field of Study    Physics

Department       Physics

Faculty           Science

Academic Year    2020

### Abstract

The ground state entanglement of the system, both in discrete-time and continuous-time cases, is quantified through the linear entropy. The result shows that the entanglement increases as the interaction between the particles increases in both time scales. It is also found that the strength of the harmonic potential affects the entanglement of the system. The different feature of the entanglement between continuous-time and discrete-time scales is that, for discrete-time entanglement, there is a cut-off condition. This condition implies that the system can never be in a maximally entangled state.

Keywords : Continuous-Time/ Discrete-Time/ Entanglement

## **ACKNOWLEDGEMENTS**

This thesis is supported by my thesis advisor, Dr. Monsit Tanasittikosol for editing and supporting my thesis writing. Next, I would like to thank another advisor, Asst. Prof. Dr for invaluable teaching and giving the motivation in my thesis. Without their advices, this thesis would not have been completed.

## CONTENTS

	<b>PAGE</b>
<b>ABSTRACT IN ENGLISH</b>	ii
<b>ACKNOWLEDGMENTS</b>	iii
<b>CONTENTS</b>	iv
<b>LIST OF FIGURES</b>	vi
<b>CHAPTER</b>	
<b>1. INTRODUCTION</b>	1
1.1 Background and motivation . . . . .	1
<b>2. THEORETICAL BACKGROUND</b>	2
<b>3. MODEL AND METHOD</b>	3
3.1 Transmission probability of electron in tilted Dirac cone . . . . .	3
<b>4. RESULT AND DISCUSSION</b>	4
4.1 Angular dependent of transmission probability . . . . .	4
4.2 The tilted strength identification by means of the tunneling resonance properties . . . . .	5
4.3 Oscillatory behavior of electron resonant tunneling . . . . .	6
4.4 Revisit: The tilted strength identification by means of the tunneling resonance properties . . . . .	7
4.5 Pseudo magnetic field . . . . .	8

	<b>PAGE</b>
4.6 Transmission under the influence of pseudo magnetic field . . . . .	9
4.7 The key consequence of the mismatch effect . . . . . . . . . . .	10
<b>5. CONCLUSION</b>	<b>11</b>
<b>REFERENCES</b>	<b>12</b>
<b>BIOGRAPHY</b>	<b>13</b>

## LIST OF FIGURES

FIGURE	PAGE
2.1 The device structure of field-effect transistor. . . . .	2
4.1 The same cup of coffee. Two times. . . . .	5
4.2 tp fixed angle . . . . .	7
4.3 (a) The device structure for the measurement of resonant tunneling electron. Straight blue lines represent the transport region where both arms are $45^\circ$ angled with the normal direction. Green and yellow region represents top gate and electrode respectively. (b) Angular-dependent transmission for different applied voltages, $U=180.2$ meV for solid line and $U=185.85$ meV for dashed-dotted line. These voltages satisfy the resonance condition at $\phi = \frac{\pi}{4}$ . . . . .	8
4.4 The polar plot of transmission probabilities as a function of incident angle of the system with tilted mismatch Dirac cone (solid line) and non-tilted system under the influence of delta magnetic field (dashed line). The Fermi energy $E_F = 83$ meV is the same for all plot, the gate potential $U = 285$ meV for (a) and (b), $U = 0$ for (c) and (d) .	10

# **CHAPTER 1 INTRODUCTION**

## **1.1 Background and motivation**

The electronic properties of material are defined by the ability of charge carriers to move throughout the crystal structures [1]

The ability of charge carriers to tunnel throughout the material is defines by the crystal, electronic structures of their host material.

## CHAPTER 2 THEORETICAL BACKGROUND

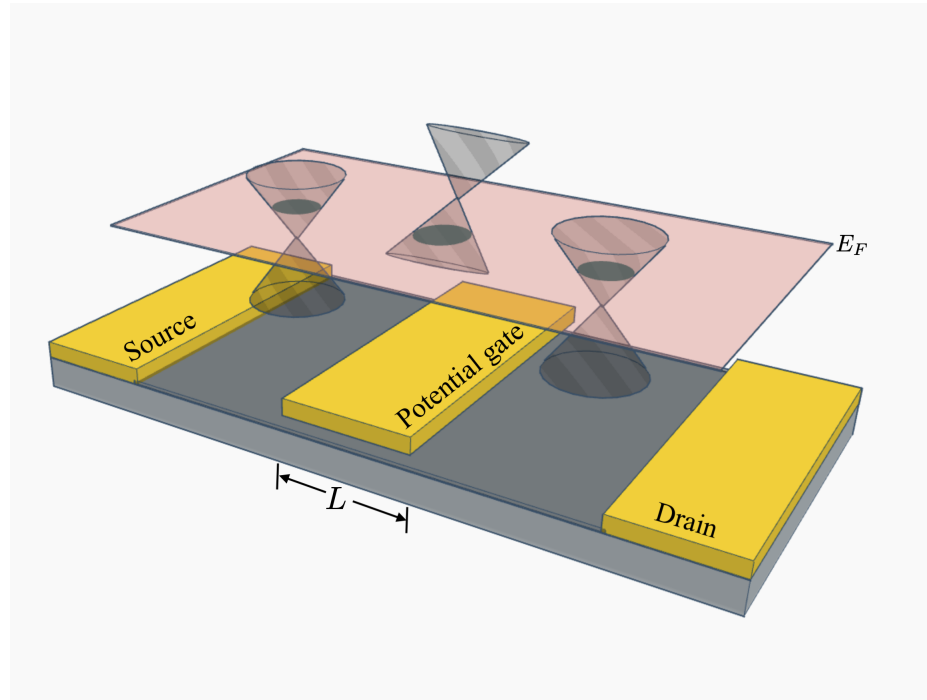


**Figure 2.1** The device structure of field-effect transistor.

## CHAPTER 3 MODEL AND METHOD

### 3.1 Transmission probability of electron in tilted Dirac cone

$$\psi_1 = \begin{cases} e^{ik_x x} + r e^{-ik_x x} & , x < 0 \\ s(e^{ik_x x} e^{i\phi} + r e^{-ik_x x} e^{-i\phi}) & , x < 0 \end{cases} \quad (3.1)$$

$$\psi_2 = \begin{cases} a e^{iq_x x} + b e^{-iq_x x} & , 0 \leq x < L \\ s'(a e^{iq_x x} e^{i\theta} - b e^{-iq_x x} e^{-i\theta}) & , 0 \leq x < L \end{cases} \quad (3.2)$$

$$\psi_3 = \begin{cases} t e^{ik_x x} & , x \geq L \\ s t e^{ik_x x} e^{i\phi} & , x \geq L \end{cases} \quad (3.3)$$

(3.4)

$$T = \frac{\cos^2 \theta \cos^2 \phi}{\cos^2(Lq_x) \cos^2 \theta \cos^2 \phi + \sin^2(Lq_x)(1 - ss' \sin \theta \sin \phi)^2} \quad (3.5)$$

## CHAPTER 4 RESULT AND DISCUSSION

We start by investigating the tunneling properties of electron across tilted Dirac cone heterojunctions where we focus on how the effect of the gate potential and tilt affect the electron transmission. Then, we demonstrate a method to measure the tilted strength of the Dirac cone by identifying the tunneling behavior. Finally, we show that the transport behaviors of electron in tilted Dirac cone material are analogous to electron under the influence of magnetic field. We also show the derivation of magnetic field strength as a function of gate potential and tilted parameter.

The calculation of transmission probability is carried out using Eq. 3.5

### 4.1 Angular dependent of transmission probability

The transmission probabilities across the tilted Dirac cone heterojunctions under the variation of gate potential are presented in Fig. 4.1. The transmission profiles are symmetric in the case of  $w_0 = 0$  regardless of the gate potential. When the tilted parameter is non-zero, the transmission profiles are shifted along the direction of the tilt and consequently become asymmetric, where the magnitude of the shift depends on the tilted strength of the Dirac cone. However, the present of the tilt barely affects the tunneling profiles when the applied gate potential is close to the Fermi energy as shown in Fig. 4.1b. This is because the Fermi surface is small and the allowed wavevector states are narrowed. Therefore, electron propagations other than the normal incident are backscattered.

Interestingly, when the applied gate voltage  $U$  is larger than the Fermi energy  $E_F$ , the transmission profiles exhibit peak tunneling as shown in Fig. 4.1c-d. These kind of tunnelings are called resonant tunneling, which occurred when the condition  $q_x L = n\pi$ ,  $n = 0, \pm 1, \dots$  in Eq. 3.5 is met.

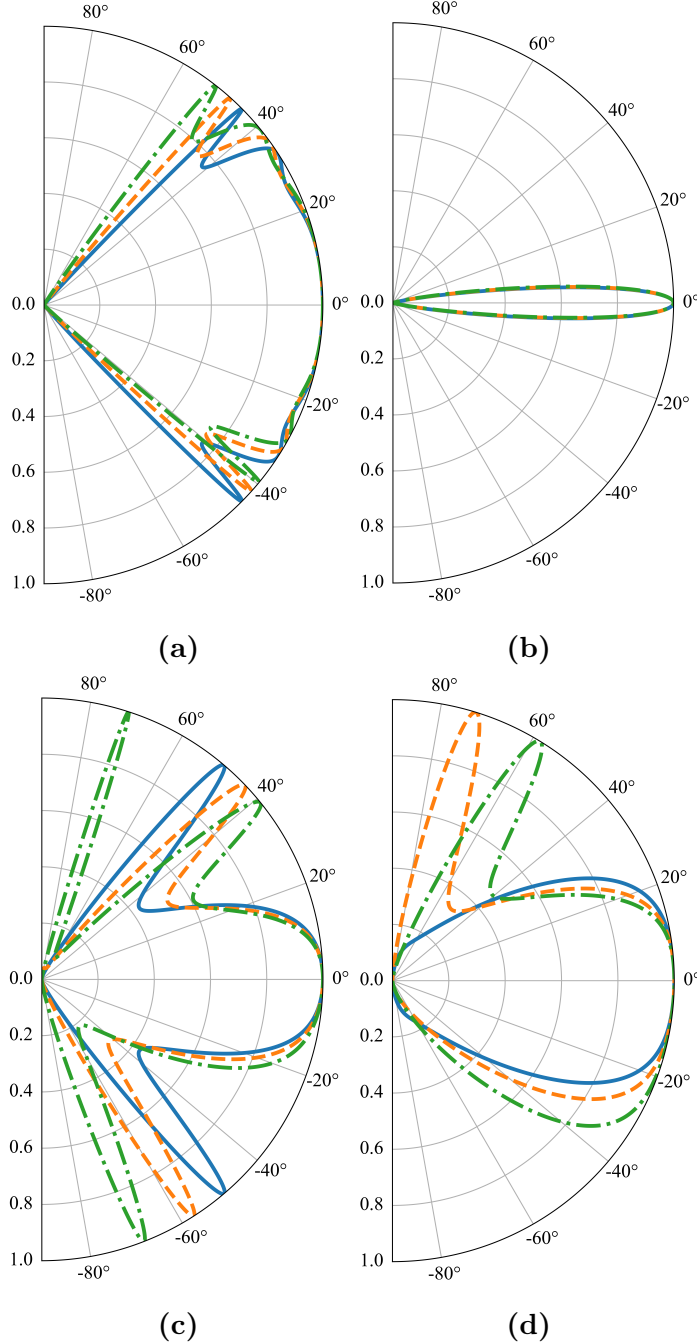


**Figure 4.1** The same cup of coffee. Two times.

## 4.2 The tilted strength identification by means of the tunneling resonance properties

The resonant tunnelings are arisen if the given  $U, E_F$  and,  $w_0$  satisfy the resonance condition. Modulating these parameters result in shifting of resonant tunneling angles as previously reported in section 4.1. In this section, we demonstrate that by measuring the asymmetric resonant tunneling angles, the tilted parameter can be

determined. Consider the resonance condition

$$\begin{aligned} L \sqrt{\left( \frac{E_F - U}{\hbar v_F} + w_0 k_y \right)^2 - k_y^2} &= n\pi \\ w_{0\pm} &= \frac{U - E_F}{\hbar v_F k \sin \phi} \mp \sqrt{1 + \left( \frac{n\pi}{kL \sin \phi} \right)^2} \end{aligned} \quad (4.1)$$

where subscript  $+(-)$  satisfy the positive(negative) angle  $\phi$  region. One can obtain the tilted parameter by applying the gate voltage and Fermi energy then measure the resonant tunneling angle, which can be experimentally observed by four-point probes technique [2]. To illustrate how to calculate for the tilted parameter, we substitute the configuration of dashed-dotted line in Fig. 4.1c to Eq. 4.1. We choose the resonance condition  $n = 4$ , which corresponds to the resonant tunneling angle  $\phi = 72^\circ$ . We find  $w_0 = 0.1$ .

However, this method is not at all practical since the variable  $n$  is unlikely observable. Also, the only way to manipulate the electron propagations is by tuning the voltages through the bottom and top gate. In section 4.4, we propose a more practical method to identify the tilted strength, which again, involve with the resonant tunneling behaviors.

### 4.3 Oscillatory behavior of electron resonant tunneling

To understand the behaviors of resonant tunneling under the effect of the tilt and gate potential, we plot the transmission probabilities at particular incident angle  $\phi = 45^\circ$  shown in Fig. 4.2. We found that the resonant tunneling oscillate with the increasing of gate voltage where the voltage difference between each resonance condition is the same. Also The voltages required to satisfy the resonance conditions are increased with the tilted strength. These resonant tunnelings are shifted uniformly with the tilted parameter, which can be confirmed mathematically by taking the derivative to Eq. 4.1 with respect to  $U$

$$\begin{aligned} \frac{dw_{0\pm}}{dU} &= \frac{d}{dU} \left( \frac{U - E_F}{\hbar v_F k \sin \phi} \mp \sqrt{1 + \left( \frac{n\pi}{kL \sin \phi} \right)^2} \right) \\ &= \frac{1}{\hbar v_F k \sin \phi}. \end{aligned} \quad (4.2)$$

Eq. 4.2 indicates that the tilted parameter is linearly proportional to gate voltage

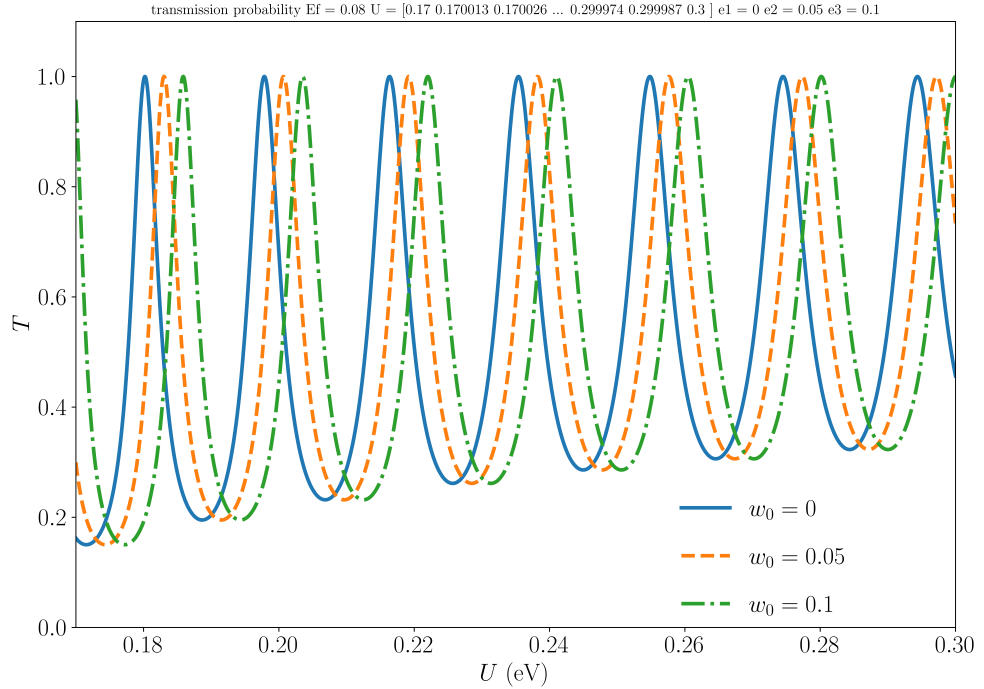


**Figure 4.2** tp fixed angle

#### 4.4 Revisit: The tilted strength identification by means of the tunneling resonance properties

In section 4.2, we have demonstrated a method to identify the character of Dirac cone using the resonant tunneling properties. The method can be applied to any resonance condition given that we have known its corresponding resonant tunneling angle. However, it is still not a practical method since the parameter  $n$  is unobservable. Also, most device configurations have fixed angled probes to observe the resonant tunneling current. In this section, we revisit this study again and eliminate the drawbacks mentioned above.

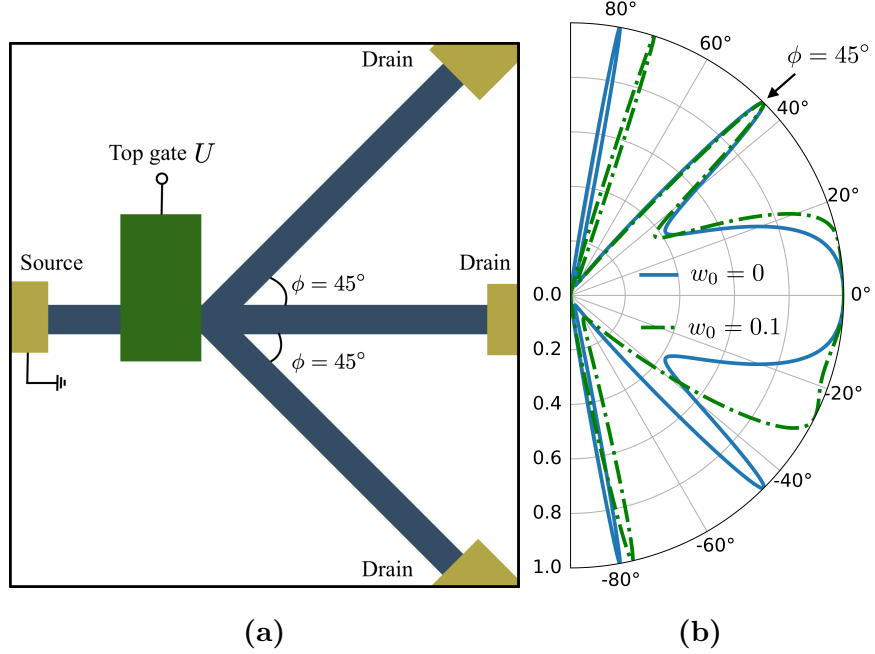


**Figure 4.3** (a) The device structure for the measurement of resonant tunneling electron. Straight blue lines represent the transport region where both arms are  $45^\circ$  angled with the normal direction. Green and yellow region represents top gate and electrode respectively. (b) Angular-dependent transmission for different applied voltages,  $U=180.2$  meV for solid line and  $U=185.85$  meV for dashed-dotted line. These voltages satisfy the resonance condition at  $\phi = \frac{\pi}{4}$ .

## 4.5 Pseudo magnetic field

In section 4.1, we have shown that the tunneling behavior of electron across the tilted Dirac cone exhibits asymmetric transmission. Previously, the transmission of this kind can be achieved by applying the magnetic barrier to the system [3, 4]. In this section, we demonstrate that the similar transmission profile can also be achieved in the tilted Dirac cone system without the magnetic barrier. Consider the x-component wavevector inside the barrier region  $q_x = \sqrt{q^2 - k_y^2}$ , which can be rearranged into the form

$$q_x \approx \sqrt{q'^2 - (k_y - q'w_0)^2} \quad (4.3)$$

where  $q' = \frac{E_F - U}{\eta \hbar v_F}$ . Notice that the y-component wavevector in Eq. 4.3 is shifted by the tilted Dirac cone similar to the wavevector shift by the effect of magnetic vector

potential. Based on this analogy, we can derive the equivalent pseudo magnetic field

$$\begin{aligned} -q'w_0 &= \frac{\xi}{l_B} \\ -\left(\frac{E_F - U}{\eta\hbar v_F}\right) w_0 &= \xi\sqrt{\frac{|e|B}{\hbar}} \\ B &= \left(\frac{\varepsilon w_0}{v_F}\right)^2 \frac{1}{\xi\gamma\hbar|e|} \end{aligned} \quad (4.4)$$

where  $\varepsilon = E_F - U$  is effective Fermi energy.  $\xi = \pm 1$  is in fact the direction of magnetic field, but since these fields are induced by the tilted Dirac cone, it can be considered as the direction of the tilt. The positive(negative) sign mean that the Dirac cone tilted to the left(right) side with respect to normal direction.  $\gamma = \pm 1$  indicate the carrier type in Fermi energy level.

## 4.6 Transmission under the influence of pseudo magnetic field

To illustrate how pseudo magnetic field affects the tunneling behaviors compared to their real counterpart, the transmissions under the effect of pseudo and real magnetic fields are plotted as shown in Fig.4.4.

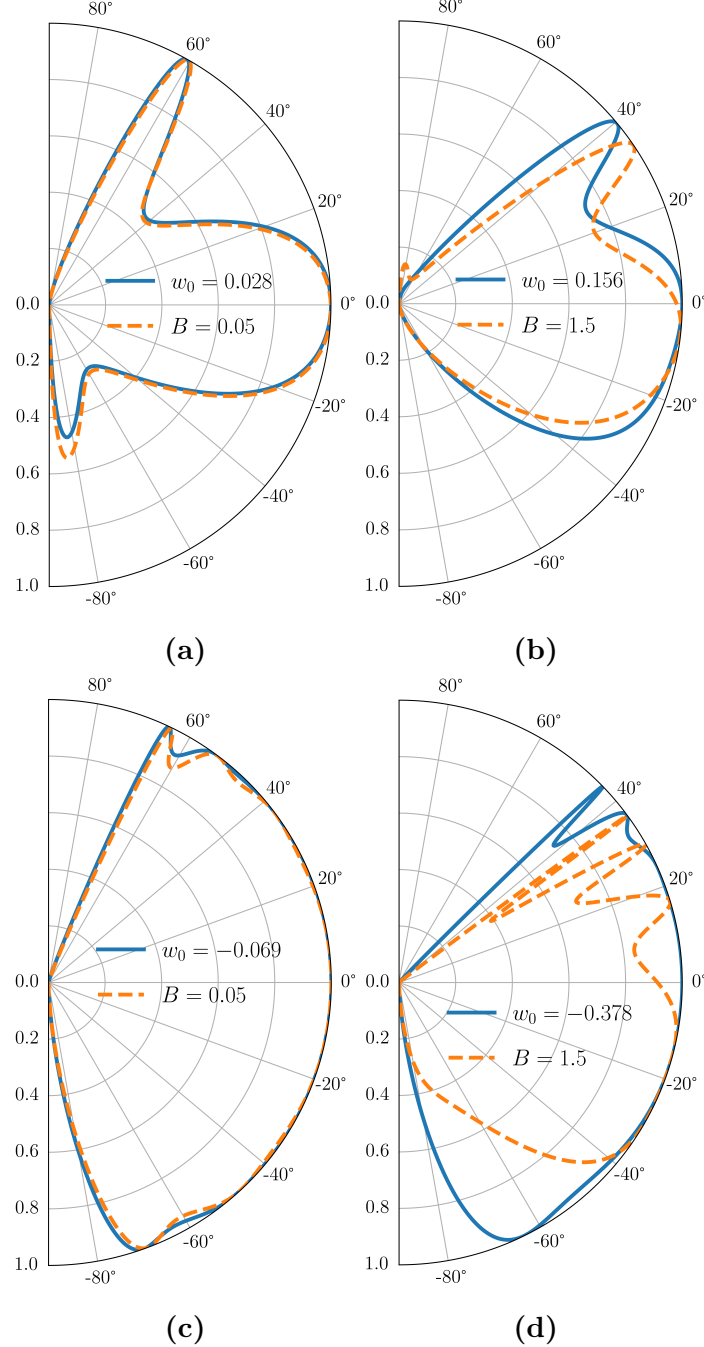


**Figure 4.4** The polar plot of transmission probabilities as a function of incident angle of the system with tilted mismatch Dirac cone (solid line) and non-tilted system under the influence of delta magnetic field (dashed line). The Fermi energy  $E_F = 83$  meV is the same for all plot, the gate potential  $U = 285$  meV for (a) and (b),  $U = 0$  for (c) and (d)

## 4.7 The key consequence of the mismatch effect

The magnetic field strength are related to the magnitude of the tilt.

## **CHAPTER 5 CONCLUSION**

The transmission probabilities of electron across tilted Dirac cone undergo the effect of pseudo magnetic field

## REFERENCES

1. K. S. Novoselov, A. K. Geim, S. V. Morozov, D. Jiang, M. I. Katsnelson, I. V. Grigorieva, S. V. Dubonos, and A. A. Firsov, “Two-dimensional gas of massless Dirac fermions in graphene,” **Nature**, vol. 438, no. 7065, pp. 197–200, nov 2005.
2. Atikur Rahman, Janice Wynn Guikema, Nora M. Hassan, and Nina Marković, “Angle-dependent transmission in graphene heterojunctions,” **Applied Physics Letters**, vol. 106, no. 1, 2015.
3. M. Ramezani Masir, P. Vasilopoulos, A. Matulis, and F. M. Peeters, “Direction-dependent tunneling through nanostructured magnetic barriers in graphene,” **Physical Review B - Condensed Matter and Materials Physics**, vol. 77, no. 23, pp. 1–11, 2008.
4. M. Ramezani Masir, P. Vasilopoulos, and F. M. Peeters, “Fabry-Pérot resonances in graphene microstructures: Influence of a magnetic field,” **Physical Review B - Condensed Matter and Materials Physics**, vol. 82, no. 11, pp. 1–12, 2010.

# CURRICULUM VITAE

**NAME** Mr. Eakkarat Pattrawutthiwong

**DATE OF BIRTH** 26 April 1995

## EDUCATIONAL RECORD

**HIGH SCHOOL** High School Graduation

Kaen Nakhon Wittayalai School, 2014

**BACHELOR'S DEGREE** Bachelor of Science (Applied Physics)

King Mongkut's University of Technology Thonburi,  
2018

**MASTER'S DEGREE** Master of Science (Physics)

King Mongkut's University of Technology Thonburi,  
2020

**PUBLICATION** Soodchomshom, B., Niyomsoot, K.,

Pattrawutthiwong, E, "Switching effects and spin-valley Andreev resonant peak shifting in silicene superconductor," **Physica E: Low-dimensional Systems and Nanostructures**, vol 97, pp. 375-383, 2018